JOURNAL OF CATALYSIS 102, 257–265 (1986)

In Situ X-Ray Diffraction Studies over Nickel Particles Supported on Titania, Niobia, and Alumina on CO Hydrogenation Reactions

INTRODUCTION

The supported nickel catalysts have received considerable attention, both industrially and for the correlation of physical and chemical properties with performance (e.g. (*1–7*)). Perhaps the attractive fact is that nickel particles are more active when supported on titania and niobia than on alumina and silica over methanation and Fischer–Tropsch synthesis. In addition, titania and niobia supported nickel catalysts show greater selectivities for the production of high hydrocarbons (*1, 2, 5–7*). Therefore previous research works were focused on exploration of the nature of interactions between nickel and different supports (*1, 2, 5–7*). Besides, several research groups have utilized *in situ* magnetic techniques for characterization of supported catalysts (*3, 8–10*). Richardson and Desai (*10*) have used ultrahigh magnetic field measurements on 40% Ni/Al_2O_3. They have pointed out that about 50% available nickel particles had been reduced in H_2 treatment (e.g., 36 hr at 350°C), even though, after 72 hr treatment, no further nickel reduction had occurred. However, the information of partially reduced nickel oxides studied by *in situ* X-ray diffraction is not well known on supported nickel catalysts.

Butt *et al.* (*12*) have directly examined the formation of palladium hydride by *in situ* X-ray diffraction over Pd/Al_2O_3 and Pd/SiO_2. In some cases an observed decrease in activity could be due to palladium hydride formation, especially for hydrogenolysis reactions (*12*). Now it is imperative to explore whether the analogous situation will occur on supported nickel catalysts.

The present study has been undertaken in an attempt to examine the presence of the different kinds of intermediate phases after H_2 reduction and CO/H_2 reaction over nickel supported titania, niobia, alumina, and ground glass, and to explore the conditions for its formation and disappearance. An *in situ* X-ray diffraction technique has been employed for this purpose. Meanwhile the determination of nickel particle sizes after reduction and CO/H_2 reaction has been made by using Fourier analysis of a single X-ray diffraction profile. A comparison of the nickel particle sizes determined by one peak analysis and high resolution transmission electron microscopy has been given.

EXPERIMENTAL

Materials and Catalyst Preparation

All catalysts used in this study were prepared by the method of incipient wetness impregnation using $Ni(NO_3) \cdot 6H_2O$ as the metal salt. In this method, TiO_2, Nb_2O_5, Al_2O_3, and ground glass were impregnated with the appropriate concentration of nickel nitrate aqueous solution in a ratio of 0.25 ml/g TiO_2, 0.4 ml/g Nb_2O_5, 0.5 ml/g Al_2O_3, and 0.3 ml/g glass. Following impregnation, all samples were dried overnight in air at ca. 380 K.

The TiO_2 support used in this study was obtained from Degussa (P-25), and it was cleaned prior to sample preparation in the manner described by Munuera *et al.* (*13*) and Santos *et al.* (*14*). The powder of ground glass was made of Pyrex-type glass material from Shanghai. Two other supports used here were spectroscopically

0021-9517/86 $3.00

pure niobia and 80/100 mesh γ-Al_2O_3 (Davison, SMR-7).

Hydrogen (99.9%) was purified by passage through a Deoxo unit followed by activated 5A and 13X molecular sieve traps at room temperature. Carbon monoxide (99.5%) was passed through two copper turnings at ca. 600 K followed by activated molecular sieves (5A and 13X) at room temperature.

In Situ X-Ray Diffraction Measurements

A specially constructed reaction cell as shown in Fig. 1 was designed for *in situ* X-ray diffraction studies. The cell was composed of two sections: one was a tubular section made of Pyrex tubing (35 mm in diameter); the other was an X-ray diffraction measurement section composed of a beryllium front window (0.2 mm thickness, 28 × 26 mm^2 wide) sealed with a "Torr seal" to the stainless-steel shell (45 × 35 × 1.5 mm^3) which was attached to the tubular section with a "Torr seal." Then, the two sections were linked by a pair of rods (stainless steel). The sample (ca. 0.25 mg) was pressed into pellet form under pressure of about 200 kPa. A pellet of catalyst was mounted on a movable sample holder which could slide from one section to another for reaction or X-ray diffraction measurements.

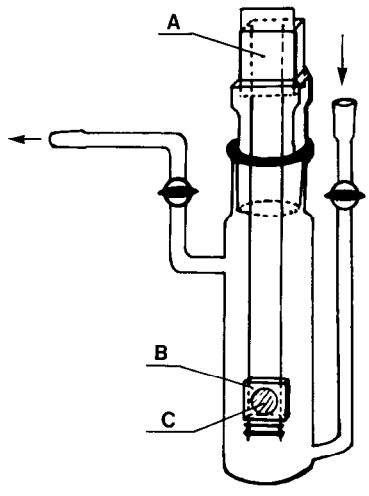

FIG. 1. Schematic diagram of a specially constructed cell. (A) Beryllium window, (B) movable sample holder, (C) sample.

The hydrogen reduction and CO/H_2 reaction were carried out at atmospheric pressure. The catalyst pellet was treated in the tubular section as a fluidized bed. After reduction or reaction the sample was cooled to room temperature under flowing H_2. Then closing the two check-valves on the cell, the sample holder was slid to another section, ready for X-ray diffraction measurements. The X-ray diffraction studies on the catalyst after reduction and/or CO/H_2 reaction were performed with Ni-filtered Cu$K\alpha$ radiation from a 12-kW Rigaku rotating anode X-ray source operated at 45 kV and 50 mA. The different scan speeds were chosen: 2°/min (or 4°/min) for recording diffraction patterns from 20°(2θ) to 95°(2θ); however, 0.25°/min for slow scan of Ni(200) and Ni(220) peak profiles in order to determine the particle sizes by single peak analysis method. After exposing the sample to air, of course, the measurements were done in air. The nickel powder sample with large particle size was employed as "standard" for calibration in calculation of nickel particle sizes of catalyst samples by one peak analysis method.

Particle Size Measurements

Usually the broadening of the X-ray diffraction profile was mainly due to the following three factors: particle size, instrumental, and microstrain. In order to obtain the pure diffraction profile broadening attributed to particle size only, it is required to separate the diffracted profile shape broadening due to both instrumental and microstrain factors. The method of Stokes (*15*) was the best approach for the correction of instrumental factor. According to the Stokes method, however, the corrected cosine coefficient from a (*hkl*) diffraction profile is really the product of two terms (*16, 17*): one involving the crystallite size and the other the microstrains. Therefore it is necessary to separate the micro-

strain from cosine coefficient in order to determine the crystallite sizes. In the present study a single analysis method had been employed for separation of the effects of the particle size and microstrains (*18, 19*).

Transmission electron microscopy studies of these catalysts after CO/H_2 reactions and exposure to air were performed using a JEOL 200CX microscope. The microscope was operated at 200 kV with a 30-μm objective aperture inserted for contrast. Magnifications were calibrated using carbon replica gratings. The samples were prepared for microscopic analysis by adding the powdered sample to methanol, grinding the suspension in a mortar and pestle, and dispersing the sample in the methanol using an ultrasonic cleaner. A drop of this suspension was then placed onto a Formvar film supported on a copper grid. As a comparison, the blank TiO_2, Nb_2O_5, and Al_2O_3 were also studied by TEM under the same operating conditions.

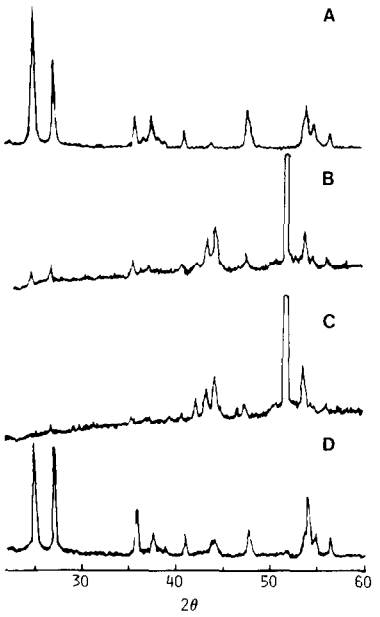

FIG. 2. X-Ray diffraction patterns over 13% Ni/TiO_2. (A) Before reduction; (B) after reduction (H_2, 700 K, 2.5 hr), then cooling to room temperature in H_2; (C) after CO/H_2 reaction (H_2/CO = 4, 500–560 K, 4 hr), then cooling to room temperature in H_2; (D) after exposing the sample to air for 8 min.

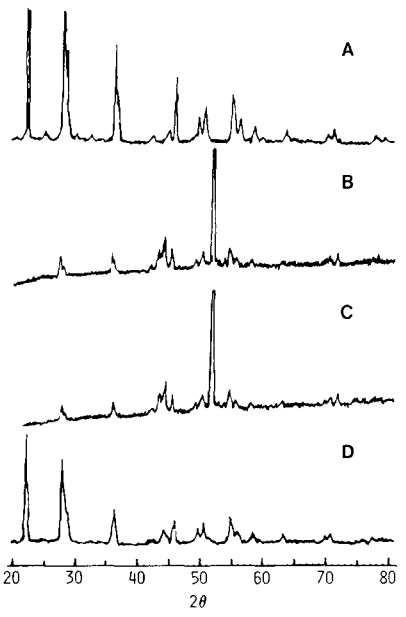

FIG. 3. X-Ray diffraction patterns over 12.5% Ni/Nb_2O_5. (A) Before reduction; (B) after reduction (H_2, 700 K, 2.5 hr), then cooling to room temperature in H_2; (C) after CO/H_2 reaction (H_2/CO = 4, 500–560 K, 4 hr), then cooling to room temperature in H_2; (D) exposure to air for ca. 2 hr.

In addition, product analysis for CO/H_2 ($\frac{1}{4}$) reactions over these catalysts were performed on a Shimadzu GC-7A chromatograph equipped with a Chromsorb 102 column (2 m long). Both flame ionization detector (FID) and thermal conductivity detector (TCD) were used for analysis. The helium carrier gas was purified by passage through an activated 13X molecular sieve trap at room temperature. The peak areas of the chromatogram were calculated by a Shimadzu C-R1B recording data processor.

RESULTS AND DISCUSSIONS

In Situ X-Ray Diffraction Measurements

The diffraction patterns on 13% Ni/TiO_2, 12.5% Ni/Nb_2O_5, and 9% Ni/Al_2O_3 are presented in Figs. 2, 3, and 4, respectively. Figures 2A, 3A, and 4A show the diffraction profiles on these samples before reduction. The titania support contains two crystalline phases: anatase and rutile. The niobia support shows single crystalline phase. The

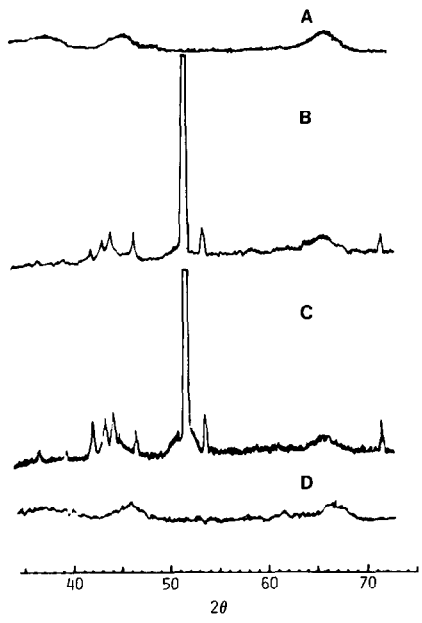

FIG. 4. X-Ray diffraction patterns over 9% Ni/Al_2O_3. (A) Blank alumina; (B) after reduction (H_2, 700 K, 2.5 hr), then cooling to room temperature in H_2; (C) after CO/H_2 reaction (H_2/CO = 4, 500–600 K, 4 hr), then cooling to room temperature in H_2; (D) exposure to air for ca. 2 hr.

alumina, however, shows mainly the amorphous phase which will be very useful in this study, because it does not interfere appreciably with diffraction peaks of other crystalline phases. The diffraction patterns obtained after hydrogen reduction at 700 K for 2.5 hr on these samples are shown in Figs. 2B, 3B, and 4B. The observation of a new phase is the key result in the present study. The formation of the intermediate phase occurred just after hydrogen reduction. Meanwhile the support phases appeared with obviously lowering the intensities of their diffraction peaks. Following reduction the CO/H_2 ($\frac{1}{4}$) reaction was carried out in the special reactor at atmospheric pressure. The reaction conditions and product distribution over these three catalysts are summarized in Table 1. Therein the CO conversion was approximately 30% or less in this special X-ray diffraction cell. The catalytic activities for methane production in Ni/TiO_2 and Ni/Nb_2O_5 are greater than that on Ni/Al_2O_3 by about a factor of 2. The selectivity of high hydrocarbons of nickel on titania and niobia supports is higher than that on alumina support as shown in Table 1. These results are consistent with previous reports (*1, 2, 7*). Figures 2C, 3C, and 4C show the diffraction patterns collected after CO/H_2 ($\frac{1}{4}$) reactions followed by cooling to room temperature under hydrogen. It

TABLE 1

The Pretreatment Conditions Used for *in Situ* X-Ray Diffraction Measurements and Product Distributions over CO Hydrogenation on Nickel Supported Catalysts

Catalyst	Reduction conditions	Reaction conditions	r_{CH_4}[a] (μmol/min g Ni)	Product distribution (mole %)[b]					
				C1	C2	C3	C4	C5	C6
13% Ni/TiO_2	H_2 (200 ml/min) 700 K, 2.5 hr	H_2/CO = 4 500–560 K 4 hr	280	54.6	12.8	11.1	6.8	8.9	5.8
12.5% Ni/Nb_2O_5	H_2 (200 ml/min) 700 K, 2.5 hr	H_2/CO = 4 500–560 K 4 hr	300	68.1	11.4	10.2	6.0	4.3	—
9% Ni/Al_2O_3	H_2 (200 ml/min) 700 K, 2.5 hr	H_2/CO = 4 500–600 K 4 hr	145	99.82	0.17	0.01	—	—	—

[a] Reaction temperature: 503 K.
[b] Reaction temperature: 503 K for 13% Ni/TiO_2 and 12.5% Ni/Nb_2O_5 and 600 K for 9% Ni/Al_2O_3.

can be seen there that the diffraction intensities of the intermediate phase did not obviously change after CO hydrogenation reaction at 500–600 K for 4 hr. In Fig. 4C the diffraction profile of the intermediate phase can be observed more clearly because of almost no interference between the new phase and the original amorphous support phase. In order to detect the stability of the so-called intermediate phase formed during hydrogen reduction, the sample 13% Ni/TiO_2 was exposed to air for several minutes (ca. 8 min), then the diffraction pattern was registered at a scan speed of 4°/min as shown in Fig. 2D, wherein it is interesting to note that the intermediate phase disappeared immediately, indicating that it is very unstable in air. However, the titania support (involving both anatase and rutile) recovered the intensities of diffraction peaks as original when the intermediate phase disappeared. Analogously Figs. 3D and 4D show the diffraction profiles obtained after exposure to air over 12.5% Ni/Nb_2O_5 and 9% Ni/Al_2O_3, respectively. The same conclusions can be drawn that the condition of the disappearance of so-called intermediate phase formed in hydrogen reduction is in contact with air and the diffraction intensities of the crystalline phase of supports recovered dramatically when the intermediate phase did not occur.

Here it is necessary to address the diffraction patterns of 9% Ni/Al_2O_3 (i.e., Fig. 4) because the blank support presents as an amorphous phase as shown in Fig. 4A. The so-called intermediate phase (including nickel suboxide phase) will be seen clearly in Figs. 4B and C, especially in Fig 4C (after CO/H_2 ($\frac{1}{4}$) reaction). With the exception of three peaks of bulk metallic nickel (i.e., 44.6(2θ){111}, 51.8(2θ{200}, and 76.4(2θ){220}), the d spacing values and relative intensities of the rest of the diffraction peaks attributed to the intermediate phase (or phases) are listed in Table 2. It will be necessary to determine the structure of the new phase in further studies.

For comparison with nickel supported on titania, niobia, and alumina, *in situ* X-ray diffraction patterns obtained after hydrogen reduction at 770 K for 1.5–3 hr followed by cooling to room temperature in hydrogen over ~10% Ni/ground glass are presented in Fig. 5. Figures 5A and B show the X-ray diffraction patterns of two fresh samples with different time periods of hydrogen treatment (i.e., 1.5 or 3 hr), wherein no intermediate phase was observed with the exception of three strong diffraction peaks of reduced metallic nickel (Ni(111), Ni(200), and Ni(220)).

As shown in Figs. 2B, 3B, 4B, 2C, 3C, and 4C the most striking observation of this study is that the presence of so-called intermediate phase (or phases) formed after hydrogen reduction and CO/H_2 ($\frac{1}{4}$) reactions. This is probably due to the phase (or phases) of partially reduced nickel oxide (or oxides). This finding is essentially consistent with previous reports by *in situ* magnetic susceptibility (*8–10*). Could it be a nickel hydride as in the case of palladium hydride formed after hydrogen treatment over Pd/SiO_2 (*12*)? For supported nickel catalysts we do not think this is the case. Of course, further studies are needed. Furthermore, supported nickel catalysts are also different

TABLE 2

d Spacing Values and Relative Intensities of the Intermediate Phase(s)

Line No.	2θ (°)[a]	d (Å)	I/I_0
1	22.7	3.914	6
2	26.7	3.336	7
3	37.1	2.421	10
4	39.8	2.263	8
5	42.5	2.215	25
6	46.9	1.936	14
7	52.2	1.751	100
8	53.9	1.694	25
9	72.0	1.310	20
10	78.3	1.220	7
11	82.1	1.173	6
12	87.5	1.132	8
13	90.9	1.081	7

[a] Nickel-filtered Cu$K\alpha$ radiation.

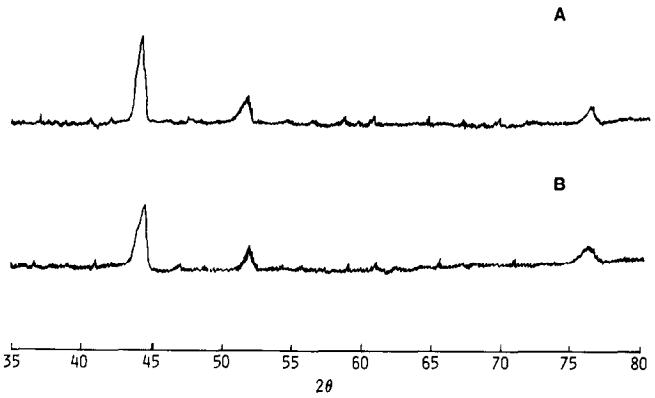

FIG. 5. X-Ray diffraction patterns over ~10% Ni/ground glass. (A) After reduction (H_2, 700 K, 1.5 hr), then cooling to room temperature in H_2; (B) after reduction (H_2, 700 K, 3 hr), then cooling to room temperature in H_2.

from the cases of production of the nickel hydrides from nickel saturation with hydrogen atmosphere or from cathodic charging or deposition as reported by Janko *et al.* (*20, 23*).

The other interesting result is that with the presence of partially reduced nickel oxide (or oxides) the diffraction intensities of crystalline phases of the supports were obviously depressed, whereas with the disappearance of so-called intermediate phases their diffraction intensities recovered dramatically. The question is what causes this apparent suppression of diffraction intensities of the supports' phases. It may be attributed to the formation of partially reduced nickel oxide (or oxides) as "interstitial" phase which, therefore, will affect the original crystalline phases of supports. Besides, from the results obtained on the sample of ~10% Ni/ground glass, there is no observation of the phase of partially reduced nickel oxide. Presumably the presence of the phase (or phases) of partially reduced nickel oxide (or oxides) implies the interaction manner between nickel particles

TABLE 3

Crystallite Sizes on Titania, Niobia, and Alumina Supported Nickel Catalysts

Sample:	13% Ni/TiO_2			12.5% Ni/Nb_2O_5			9% Ni/Al_2O_3		
Crystallite size (nm)	$D_{\text{one-peak}}$[a]		D_{TEM}[b]	$D_{\text{one-peak}}$		D_{TEM}	$D_{\text{one-peak}}$		D_{TEM}
	Ni (200)	Ni (220)		Ni (200)	Ni (220)		Ni (200)	Ni (220)	
After reduction[c]	—	13	—	—	14	—	8	9	—
After CO hydrogenation[d]	—	—	—	—	15	—	—	9	—
Exposure to air	13	12	12	—	15	15	8	9.5	8

[a] Effective particle size from profile analysis.

[b] Average particle size from transmission electron microscopy (TEM).

[c] Reduction conditions: H_2 (200 ml/min), 700 K, 2.5 hr.

[d] Reaction conditions: $H_2/CO = 4$, 3 hr, 500 K for 13% Ni/TiO_2 and 12.5% Ni/Nb_2O_5 and 600 K for 9% Ni/Al_2O_3.

and supports. It seems that there is no interaction between nickel particles and ground glass; thus the partially reduced nickel oxide (or oxides) was not observed on the sample of ~10% Ni/ground glass, as shown in Fig. 5. We speculate that this interaction manner may modify the catalytic properties of nickel supported on titania, niobia, and alumina. However, the difference in catalytic activity and selectivity on CO hydrogenation over these three catalysts may be related to the reducibility of different supports as suggested by previous publications (*7, 24, 25*).

Particle Size Measurements

According to the method of a single diffraction peak Fourier analysis, the calculated nickel particle sizes (Ni(200) and Ni(220)) are given in Table 3 after H_2 reduction, CO/H_2 ($\frac{1}{4}$) reaction, and exposure to air. From the results on 12.5% Ni/Nb_2O_5 and 9% Ni/Al_2O_3 it can be seen that almost no particle size growth occurred after CO/H_2 reactions under the conditions of the present studies (Table 1).

Figures 6A and B are representative transmission electron micrographs of blank niobia and reduced 12.5% Ni/Nb_2O_5 after CO hydrogenation. It can be seen in Fig. 6B that a number of small particles were presented in the micrograph which did not appear in the corresponding blank niobia (Fig. 6A). Analogously, the similar situation can be observed in the cases of Ni/TiO_2 and Ni/Al_2O_3 samples. Figure 7 presents particle size distributions of nickel crystallites on 13% Ni/TiO_2, 12.5% Ni/Nb_2O_5, and 9% Ni/Al_2O_3 after CO/H_2 ($\frac{1}{4}$) reactions and exposure to air from transmission electron micrographs. An area-average particle size (D_{TEM}) was estimated from the sizes, d_i, of more than 100 particles using the following relation (*26*):

$$D_{TEM} = \sum_i d_i^3 \Big/ \sum_i d_i^2.$$

The results determined in this manner are listed in Table 3, wherein one can see that the values of D_{TEM} agree well with the results of the nickel particle sizes computerized by using Fourier analysis of a single X-ray diffraction profile.

CONCLUSIONS

(1) An *in situ* X-ray examination over four different supported nickel catalysts has been demonstrated.

(2) The intermediate phase (or phases) forms when the catalysts of nickel supported on titania, niobia, and alumina are cooled after reduction and/or CO/H_2 ($\frac{1}{4}$) reaction in hydrogen. There is no observation

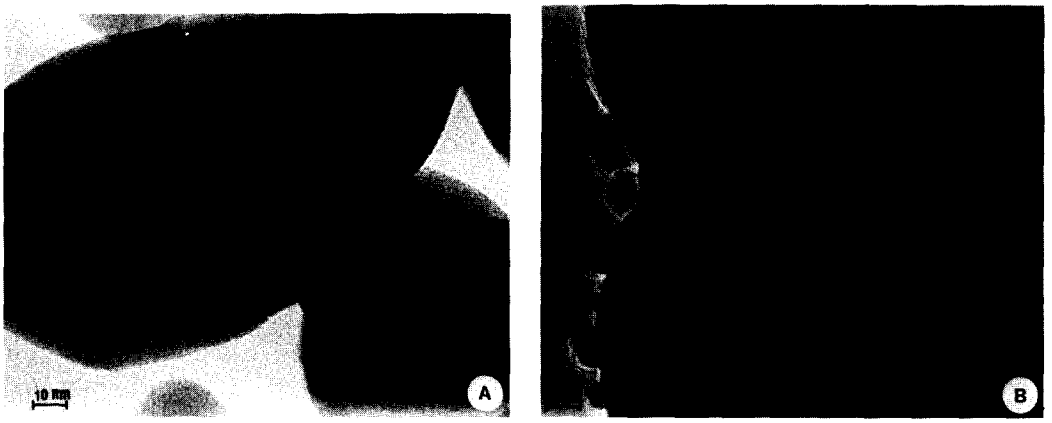

FIG. 6. Transmission electron micrograph. (A) Blank niobia; (B) reduced 12.5% Ni/Nb_2O_5 after CO hydrogenation followed by exposure of the sample to air.

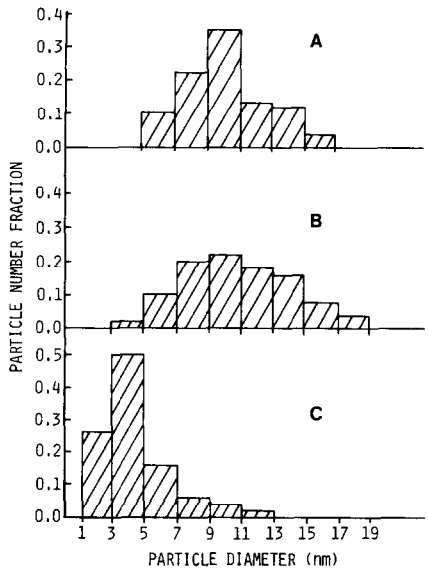

FIG. 7. Particle size distributions of nickel crystallites on (A) 13% Ni/TiO_2, (B) 12.5% Ni/Nb_2O_5, and (C) 9% Ni/Al_2O_3 after CO/H_2 ($\frac{1}{4}$) reactions and exposure to air from transmission electron micrographs.

of this phase (or phases) on nickel supported on ground glass. The formation may be related to the interaction behavior between nickel particles and the supports.

(3) The intermediate phase (or phases) which may be composed of partially reduced nickel oxide (or oxides) is destroyed in contact with air.

(4) The presence of the intermediate phase exhibits apparent suppression of the diffraction intensities of the support phases, while with the disappearance of this phase the supports show original diffraction intensities.

(5) As Fourier analysis results of a single X-ray diffraction profile show, no obvious particle size growth occurs after CO/H_2 ($\frac{1}{4}$) reactions over these catalysts.

ACKNOWLEDGMENT

We gratefully acknowledge Professor J. A. Dumesic (University of Wisconsin) for very helpful discussions.

REFERENCES

1. Vannice, M. A., and Garten, R. L., *J. Catal.* **56,** 236 (1979).
2. Bartholomew, C. H., Pannel, R. B., and Butler, J. L., *J. Catal.* **65,** 335 (1980).
3. Martin, G. A., Dutartre, R., and Dalmon, J. A., *Stud. Sci. Catal.* **4,** 467 (1980).
4. Shen, W. M., Dumesic, J. A., and Hill, C. G., Jr., *J. Catal.* **68,** 152 (1981).
5. Burch, R., and Flambard, A. R., *J. Catal.* **78,** 389 (1982).
6. Ko, E. I., Hupp, J. M., Rogan, F. H., and Wanger, N. J., *J. Catal.* **84,** 85 (1983).
7. Jiang, X. Z., Stevenson, S. A., and Dumesic, J. A., *J. Catal.* **91,** 11 (1985).
8. Martin, G. A., *J. Chim. Phys. Physicochim. Biol.* **66,** 140 (1969).
9. Martin, G. A., Ceaphalan, N., De Montgolfier, P., and Imelik, B., *J. Chim. Phys. Physicochim. Biol.* **70,** 1422 (1973).
10. Richardson, J. T., and Desai, P., *J. Catal.* **42,** 294 (1976).
11. Cale, T. S., and Richardson, J. T., *J. Catal.* **79,** 378 (1981).
12. Nandi, R. K., Pitchai, R., Wong, S. S., Cohen, J. B., Burwell, R. L., and Butt, J. B., *J. Catal.* **70,** 298 (1981).
13. Munuera, G., Moreno, F., and Gonzalez, F., *in* "Proceedings, 7th International Symposium on the Reactivity of Solids" (J. S. Anderson, M. W. Roberts, and F. S. Stone, Eds.), p. 681. Chapman & Hall, London, 1972.
14. Santos, J., Phillips, J., and Dumesic, J. A., *J. Catal.* **81,** 147 (1983).
15. Stokes, A. R., *Proc. Phys. Soc. London* **61,** 382 (1948).
16. Wagner, C. N. J., *in* "Local Atomic Arrangements Studied by X-Ray Diffraction" (J. B. Cohen and J. E. Hilliard, Eds.). New York, 1966.
17. Warren, B. E., "X-Ray Diffraction," p. 251. Addison–Wesley, 1969.
18. Gangulee, A., *J. Appl. Crystallogr.* **7,** 434 (1974).
19. Ganesan, P., Kuo, H. K., Saavedra, A., and De Angelis, R. T., *J. Catal.* **52,** 310 (1978).
20. Janko, A., *Naturwissenschaften* **47,** 225 (1969).
21. Bonisewski, T., and Smith, G. C., *J. Phys. Chem. Solids* **21,** 115 (1961).
22. Cable, J. W., Wollan, E. O., and Koehler, W. C., *J. Phys. Chem. Solids* **24,** 1141 (1963).
23. Janko, A., and Pielaszek, J., *Bull. Acad. Pol. Sci. Ser. Sci. Chim.* **15**(11), 569 (1967).
24. Tauster, S. C., *J. Catal.* **55,** 29 (1978).
25. Raupp, G. B., and Dumesic, J. A., *J. Phys. Chem. Lett.* **88,** 660 (1984).
26. Freel, J., *J. Catal.* **25,** 139 (1972).

XUAN-ZHEN JIANG[1]
BI-HAI SONG
YANG CHEN
YOU-WEN WANG

Department of Chemistry
University of Zhejiang
Hangzhou, Zhejiang
China

[1] To whom all correspondence should be addressed.

Received February 6, 1986